THE JOURNAL OF BIOLOGICAL CHEMISTRY VOL. 286, NO. 11, pp. 9298–9307, March 18, 2011

Molecular Basis and Structural Insight of Vascular K_{ATP} Channel Gating by *S*-Glutathionylation*[S]

Received for publication, October 19, 2010, and in revised form, January 5, 2011 Published, JBC Papers in Press, January 7, 2011, DOI 10.1074/jbc.M110.195123

Yang Yang[1,2], Weiwei Shi[2,3], Xianfeng Chen[2,4], Ningren Cui, Anuhya S. Konduru, Yun Shi[5], Timothy C. Trower, Shuang Zhang, and Chun Jiang[6]

From the Department of Biology, Georgia State University, Atlanta, Georgia 30302-4010

The vascular ATP-sensitive K^+ (K_{ATP}) channel is targeted by a variety of vasoactive substances, playing an important role in vascular tone regulation. Our recent studies indicate that the vascular K_{ATP} channel is inhibited in oxidative stress via *S*-glutathionylation. Here we show evidence for the molecular basis of the *S*-glutathionylation and its structural impact on channel gating. By comparing the oxidant responses of the Kir6.1/SUR2B channel with the Kir6.2/SUR2B channel, we found that the Kir6.1 subunit was responsible for oxidant sensitivity. Oxidant screening of Kir6.1-Kir6.2 chimeras demonstrated that the N terminus and transmembrane domains of Kir6.1 were crucial. Systematic mutational analysis revealed three cysteine residues in these domains: Cys^{43}, Cys^{120}, and Cys^{176}. Among them, Cys^{176} was prominent, contributing to >80% of the oxidant sensitivity. The Kir6.1-C176A/SUR2B mutant channel, however, remained sensitive to both channel opener and inhibitor, which indicated that Cys^{176} is not a general gating site in Kir6.1, in contrast to its counterpart (Cys^{166}) in Kir6.2. A protein pull-down assay with biotinylated glutathione ethyl ester showed that mutation of Cys^{176} impaired oxidant-induced incorporation of glutathione (GSH) into the Kir6.1 subunit. In contrast to Cys^{176}, Cys^{43} had only a modest contribution to *S*-glutathionylation, and Cys^{120} was modulated by extracellular oxidants but not intracellular GSSG. Simulation modeling of Kir6.1 *S*-glutathionylation suggested that after incorporation to residue 176, the GSH moiety occupied a space between the slide helix and two transmembrane helices. This prevented the inner transmembrane helix from undergoing conformational changes necessary for channel gating, retaining the channel in its closed state.

ATP-sensitive K^+ (K_{ATP})[7] channels are expressed in a variety of tissues, including smooth muscles, pancreatic β-cells, myocardium, and neurons, where they play an important role in cellular function (1, 2). Activity of the K_{ATP} channels is tuned by physiological or pathophysiological stimuli, including hypoxia, hyperglycemia, ischemia, and oxidative stress, allowing a regulation of cellular excitability according to the metabolic state (3). The vascular smooth muscle (VSM) isoform of K_{ATP} channels regulates vascular tones (4, 5). Activation of the channel by vasodilators produces hyperpolarization of VSM cells, reduces activity of the voltage-dependent Ca^{2+} channels, and relaxes VSMs. Inhibition of the channel leads to constriction of VSMs. Disruption of the vascular K_{ATP} channel in mice results in vasospasm in coronary arteries and sudden cardiac death (6, 7).

Other studies have further shown that disruption of the vascular K_{ATP} channel has drastic effects on the systemic response to septic stress. With a forward genetic approach by genome-wide random chemical mutagenesis, Croker *et al.* (8) screened a large population of mice and found four strains that are highly susceptible to multiple septic pathogens, including lipopolysaccharides (LPSs). The LPS hypersensitivity phenotype of these mice is due to a null allele of *Kcnj8*, encoding the Kir6.1 subunit of the vascular K_{ATP} channel (8). Similar septic susceptibility has been observed in *Kcnj8*-knock-out mice that also show coronary hypoperfusion and myocardial ischemia during LPS exposure (9). These studies thus indicate that the vascular K_{ATP} channel not only contributes to the vascular tone regulation at physiological conditions but also affects critically systemic stress responses.

Our recent studies have shown that the vascular K_{ATP} channel is strongly inhibited in oxidative stress by *S*-glutathionylation (10). *S*-Glutathionylation is a post-translational modification mechanism occurring in a variety of physiological or pathophysiological conditions (11). This protein modulation mechanism is remarkable especially in vasculatures because oxidative stress is a major contributing factor to several cardiovascular diseases, in which *S*-glutathionylation plays an important role (12). Although *S*-glutathionylation is often associated with the adverse effects of oxidative stress, such a protein modulation is reversible under certain circumstances and can act as a functional modulation mechanism like protein phosphorylation (11). Thus, demonstration of how *S*-glutathionylation

* This work was supported, in whole or in part, by National Institutes of Health Grant HD060959. This work was also supported by American Heart Association Grant 09GRNT2010037.

[S] The on-line version of this article (available at http://www.jbc.org) contains supplemental Figs. 1–3 and Movie 1.

[1] A Brains and Behavior Fellow of Georgia State University.

[2] These authors contributed equally to this work.

[3] Present address: Dept. of Surgery, Carlyle Fraser Heart Center, Emory University Hospital Midtown, Emory University School of Medicine, Atlanta, GA 30308.

[4] Pathogen Discovery/GRVLB/DVD/NCIRD, Centers for Disease Control and Prevention, Atlanta, GA 30329.

[5] Present address: Dept. of Cellular and Molecular Pharmacology, University of California, San Francisco, CA 94158.

[6] To whom correspondence should be addressed: Dept. of Biology, Georgia State University, 100 Piedmont Ave., Atlanta, GA 30302-4010. Tel.: 404-413-5404; Fax: 404-413-5301; E-mail: cjiang@gsu.edu.

[7] The abbreviations used are: K_{ATP}, ATP-sensitive K^+; VSM, vascular smooth muscle; BioGEE, biotinylated glutathione ethyl ester; PDS, pyridine disulfide; 2-DTP, 2,2′-dithiodipyridine; DTNB, 5,5′-dithiobis-2-nitrobenzoic acid.

affects protein function should have broad significance. As for the vascular K_{ATP} channel *S*-glutathionylation, the molecular basis remains unclear. Therefore, we performed studies to elucidate the molecular basis of and to provide structural insight into the K_{ATP} channel *S*-glutathionylation.

MATERIALS AND METHODS

Chemicals and Reagents—Chemicals or reagents used in this study were purchased from Sigma-Aldrich unless stated otherwise. High concentration stocks were prepared in double-distilled water or DMSO. The final concentration of DMSO in the experimental solution was less than 0.1%, which did not cause any detectable effect on the channel activity.

Expression of K_{ATP} Channel—The human embryonic kidney (HEK) cell line was used for expression of the wild type (WT), chimerical, and mutant channels. HEK cells were maintained in Dulbecco's modified Eagle's medium (DMEM)/F-12 medium supplied with 10% fetal bovine serum (FBS) and penicillin/streptomycin at 37 °C with 5% CO_2. Rat Kir6.1 (GenBank™ number D42145), mouse Kir6.2 (GenBank™ number D50581) and SUR2B (GenBank™ number D86038, mRNA isoform NM_011511) cloned in pcDNA3.1 (a eukaryotic expression vector) were used for transfection. The HEK cells cultured in 35-mm Petri dishes at ~90% confluence were transfected with 1 μg of Kir6.1 (or Kir6.2, either WT, chimerical, or mutants), 3 μg of SUR2B, and 0.4 μg of green fluorescent protein (GFP) cDNA (pEGFP-N2, Clontech, Palo Alto, CA) using Lipofectamine 2000 (Invitrogen). The cells were disassociated with trypsin (0.25%) after 6–24 h of transfection and split to coverslides for further growth. Patch experiments were performed on the cells grown on the coverslips during the following 12–48 h.

Electrophysiology—Patch clamp experiments were performed according to our previous reports (13–18). Whole-cell currents were recorded in voltage clamp with a holding potential of 0 mV and a hyperpolarizing step to −80 mV. Symmetric concentrations of K^+ (145 mM in total) were applied to both bath and pipette solution. The bath solution contained 10 mM KCl, 135 mM potassium gluconate, 5 mM EGTA, 5 mM glucose, and 10 mM HEPES (pH 7.4), whereas the pipette solution had 10 mM KCl, 133 mM potassium gluconate, 5 mM EGTA, 5 mM glucose, 1 mM K_2ATP, 0.5 mM NaADP, 1 mM $MgCl_2$, and 10 mM HEPES (pH 7.4). All recordings were made with an Axopatch 200B amplifier (Axon Instruments Inc., Foster City, CA). The data were low pass-filtered (2 kHz; Bessel 4-pole filter; −3 dB) and digitized (10 kHz, 16-bit resolution) with Clampex 9 (Axon Instruments Inc.). Macroscopic currents were recorded from giant inside-out patches, and single-channel currents were recorded from regular inside-out patches with a constant single voltage of −80 or −60 mV. In the inside-out patch configurations, 1 mM K_2ATP and 0.5 mM NaADP were included in the bath solution to maintain the channel activity. A higher sampling rate (20 kHz) was used for the currents recorded from the inside-out patches. Data were analyzed using Clampfit 9 (Axon Instruments Inc.).

Mutagenesis and Construction of Chimeras—Construction of chimeras was described previously (16). Briefly, Kir6.x channels were divided into three regions (N terminus, core domain containing two transmembrane domains and the pore loop, and C terminus). For Kir6.1, the N terminus, core domain, and C terminus consisted of residues 1–71, 72–186, and 187–424, respectively. For Kir6.2, the corresponding domains were 1–70, 71–176, and 177–390, respectively. Kir6.1-Kir6.2 chimeras were created by overlap extension using a PCR with *Pfu* DNA polymerase (Stratagene, La Jolla, CA). WT Kir6.1 was named 111, and WT Kir6.2 was named 222. If the N terminus was replaced with the corresponding regions from Kir6.2, we called it 211. Similarly, if the C terminus of Kir6.1 was constructed to Kir6.2, we designated the chimerical channel 221. All possible combinations (six in total) were created and named with this nomenclature system.

Site-directed mutagenesis kits (Stratagene) were used to introduce mutations. In these experiments, two oligonucleotide primers (30–35 bp) were synthesized, each of which contained the same mutation and annealed to the same sequence on opposite strands of the cDNA. *Pfu* DNA polymerase was used to extend and incorporate the mutagenic primers, leading to two nicked circular strands. DpnI was used to digest the parental cDNA. The circular, nicked double-strained DNA was transformed to XL1-Blue competent cells for amplification. The correct constructs and mutations were confirmed by DNA sequencing.

Streptavidin Pull-down Assay and Western Blot—HEK cells expressing WT or mutant Kir6.1/SUR2B channels were used for these experiments. Cells were allowed to grow to ~80–90% confluence (about 10^6 cells) in the 35-mm dish. Before experiments, cells were incubated with fresh medium for 2 h. Biotinylated glutathione ethyl ester (BioGEE; 250 μM) (Invitrogen) then was added to the medium for a 1-h incubation followed by a 15-min H_2O_2 (750 μM) challenge. Excess free BioGEE was removed by three washes (10 min each) with PBS (containing 0.3% Triton X-100). Radioimmune precipitation assay buffer (100 μl) (Sigma) was used for cell lysis. Protein concentration was measured using a BCA protein assay system (Thermo Scientific, Waltham, MA) and ranged from 2 to 8 mg/ml in our preparation. All of the WT and mutant protein samples were diluted to 1 mg/ml so that at this time point all of the protein concentrations were comparable. For the Western blot before pull-down, 15-μl samples of both WT and mutant channels were used for immunoblotting. Samples were run on a 10% SDS-polyacrylamide non-reducing gel and then transferred to a nitrocellulose membrane (Bio-Rad). Rabbit primary antibodies against Kir6.1 (1:500) (Sigma, P0874), monoclonal antibodies against β-actin (1:5000) (Sigma, A5441), and secondary antibodies conjugated with alkaline phosphatase (1:10,000) (Jackson ImmunoResearch) were used. SuperSignal West Pico chemiluminescent substrate (Thermo Scientific) was used for signal visualization. Experiments were repeated at least four times.

Streptavidin-Dynabeads (Invitrogen, M-280) were used to pull down the biotin-GSH-conjugated proteins. Briefly, before the immobilization, the Dynabeads were washed three times (10 min each) with washing buffer to remove preservatives. Protein samples (100 μl, in a concentration of 1 mg/ml) from HEK cells expressing either WT Kir6.1 channels or C176A mutant channels were then mixed with 100 μl of Dynabeads (10 mg/ml), respectively. The mixture was then incubated at room

temperature with gentle rotation for 30 min. The Dynabead-protein complex was separated as pellet from other unlabeled proteins by a magnet. The pellet containing labeled proteins was resuspended, followed by three washes, whereas the supernatant was discarded. At last, the pellets were mixed with 20 μl of loading buffer containing 0.1% SDS for boiling to release the glutathionylated proteins into solvent. The solvent containing the pull-down samples (15 μl) was loaded to the gel for Western blot as described above. In this procedure, the same amount of protein (100 μl, 1 mg/ml) was treated with the same amount of streptavidin beads (100 μl, 10 mg/ml) for both WT and mutant channels.

The photodensity of the WT and mutant channel bands before and after pull-down was quantified by ImageJ (National Institutes of Health). The photodensity of the WT channel after pull-down was divided by the photodensity of the WT channel before pull-down (designated as R_{WT}). Similarly, the photodensity of the C176A mutant channel after pull-down was divided by the photodensity of the C176A mutant channel before pull-down (R_{MT}). R_{MT} was then divided by R_{WT} to obtain the relative (percentage) density.

Structural Modeling—The native Kir6.1 structure in its closed state was generated using the I-TASSER protein structure prediction server (19–21) with bacterial KirBac1.1 (Protein Data Bank entry 1p7b), KirBac3.1 (Protein Data Bank entry 1xl4), and prokaryotic Kir3.1 channel chimera (Protein Data Bank entry 2qks) as the templates (22, 23) and further refined with eukaryotic cKir2.2 (Protein Data Bank entry 3jyc) (24). The Kir6.1 open state structure was generated using the KirBac1.1 open state model provided by Dr. Venien-Bryan (25, 26). The native Kir6.1 structural model was further modified by incorporating the GSH molecule onto the thiol group of Cys^{176}. Several candidate locations and orientations of GSH in the Kir6.1 structural model were considered based on the interaction of charged groups of GSH with that of Kir6.1 proteins and refined using energy minimization (27). The one with the lowest binding energy between GSH and the Kir6.1 protein was chosen for further analysis and presentation. The sequence alignment was created by ClustalW2. Structural images were generated with the PyMOL molecular graphics system (DeLano Scientific, LLC, San Carlos, CA). Distances between molecules were measured with PyMOL.

Data Analysis—Data are presented as means ± S.E. Differences were evaluated with Student's *t* tests or analysis of variance, and the statistical significance was accepted when p was <0.05.

RESULTS

Subunit Identification—Functional K_{ATP} channels consist of four pore-forming Kir6.x subunits (Kir6.1 or Kir6.2) and four regulatory sulfonylurea receptors (SUR1, SUR2A, or SUR2B) (2, 4). The Kir6.1/SUR2B channel is considered to be the major vascular isoform of the K_{ATP} channels, although Kir6.2 is also found in VSM cells (28, 29). Our recent studies demonstrate that the Kir6.1/SUR2B isoform of vascular K_{ATP} channel is targeted by reactive oxygen species through *S*-glutathionylation (10). To further identify the specific subunit(s) or isoform(s) targeted by oxidants, we expressed Kir6.1/SUR2B and Kir6.2/SUR2B channels in HEK cells separately. Both Kir6.1/SUR2B and Kir6.2/SUR2B currents were activated by the specific K_{ATP} channel activator pinacidil (10 μM) and inhibited by the channel inhibitor glibenclamide (10 μM) (Fig. 1, *A* and *B*, *Glib*). The currents of interest were normalized to the window of pinacidil and glibenclamide effects.

Application of H_2O_2 caused a marked inhibition of the Kir6.1/SUR2B currents in a concentration-dependent manner (Fig. 1, *A* and *G*). In contrast, the Kir6.2/SUR2B currents were barely inhibited by H_2O_2 up to 10 mM (4.5 ± 3.3% inhibition, $n = 4$) (Fig. 1, *B* and *G*). The differential responses to oxidants between Kir6.1/SUR2B and Kir6.2/SUR2B channels were further investigated using pyridine disulfides (PDSs), pharmacological tools that react with protein cysteine residues similarly as *S*-glutathionylation (10). 2,2′-Dithiodipyridine (2-DTP) (50 μM), a membrane-permeable PDS, inhibited whole-cell Kir6.1/SUR2B currents by 95.8 ± 1.1% ($n = 5$) (Fig. 1, *C* and *H*), whereas the same concentration of 2-DTP inhibited the Kir6.2/SUR2B channel by only 12.9 ± 0.5% ($n = 4$) (Fig. 2*B*). This suggests that the critical residue(s) or domain(s) for thiol oxidation are located in the Kir6.1 subunit.

Intracellular Versus Extracellular Location—To determine the intracellular *versus* extracellular location of the *S*-glutathionylation sites, the effects of membrane-permeable and -impermeable PDSs were compared. Under the same recording conditions as for 2-DTP, a high concentration of 5,5′-dithiobis-2-nitrobenzoic acid (DTNB) (200 μM), a membrane-impermeable PDS, marginally inhibited the channel activity by 28.7 ± 5.2% ($n = 5$) (Fig. 1, *D* and *H*). These different effects of DTNB and 2-DTP were not due to different potencies of these PDSs because 2-DTP and DTNB inhibited Kir6.1/SUR2B channel activity to almost the same extent when they were applied to the internal membranes of inside-out patches (Fig. 1, *E*, *F*, and *I*). The different effects of 2-DTP and DTNB in whole-cell recording *versus* inside-out patches therefore indicate that the modulation of thiol groups takes place mainly on the intracellular side of the plasma membranes.

Determination of Critical Protein Domains—To determine the critical domains for channel inhibition, we took the advantage of the different sensitivity of the Kir6.1 and Kir6.2 to thiol oxidation and performed experiments using six Kir6.1/Kir6.2 chimerical constructs created in our laboratory (16). In these chimeras, the N terminus, transmembrane core region, and C terminus were swapped between Kir6.1 and Kir6.2. All constructs expressed functional channels with SUR2B. The responses of these chimerical channels to 2-DTP were then examined. In comparison with 222 (or Kir6.2; 12.9 ± 0.5% inhibition; $n = 4$) (Fig. 2, *A* and *B*), chimeras 122 (the N terminus of Kir6.2 was substituted with that of Kir6.1; other chimeras are named similarly) and 212 gained substantial sensitivity to 2-DTP with the N terminus or core domain from Kir6.1 (68.5 ± 6.2 and 57.6 ± 5.9% inhibition, respectively; $n = 4$; $p < 0.05$) (Fig. 2, *A*, *C*, and *D*). However, chimera 221 did not show any significant difference in its response to 2-DTP compared with 222 (Fig. 2, *A* and *E*; $p > 0.05$). Moreover, in comparison with 111 (or Kir6.1; 95.8 ± 1.1% inhibition; $n = 5$), the inhibitory effect of 2-DTP on both 211 and 121 was significantly reduced (87.4 ± 5.3 and 65.4 ± 8.2% inhibition, respectively; $n = 4$; $p <$

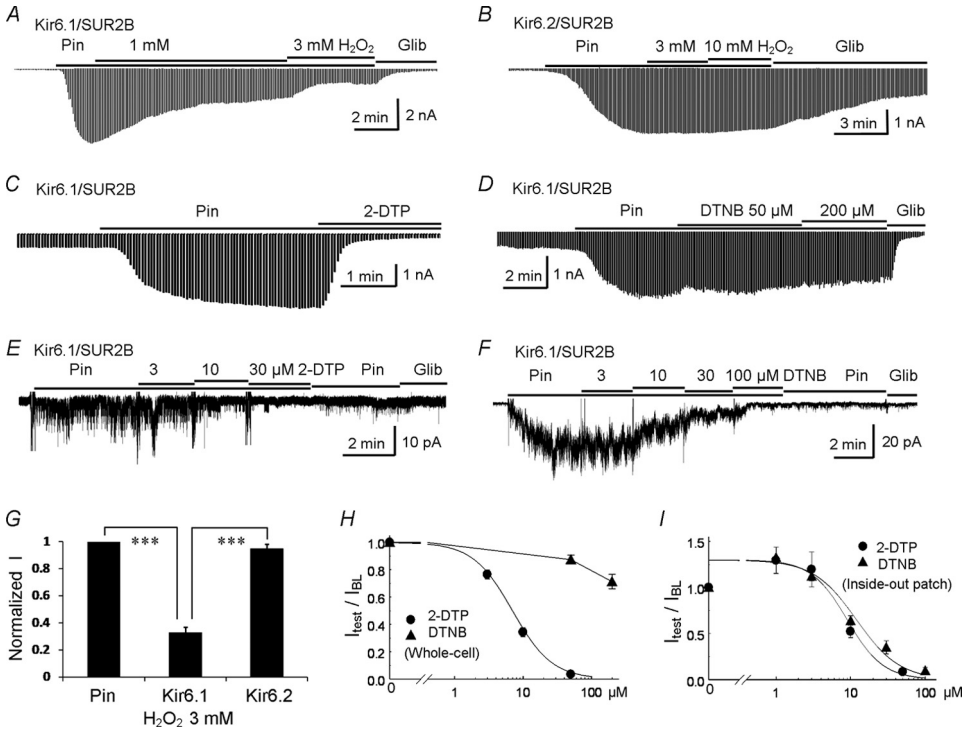

FIGURE 1. **Redox-mediated vascular K_{ATP} channel inhibition.** *A*, whole-cell voltage clamp was performed on a cell expressing the Kir6.1/SUR2B channel. The reversal potential of K^+ current was close to 0 mV by using equilibrated bath and pipette solutions containing 145 mM K^+. Command pulses of −80 mV were given every 3 s. Application of pinacidil (*Pin*; 10 μM) markedly augmented the whole-cell currents, which were subsequently inhibited by increased doses of H_2O_2 (1 and 3 mM). Glibenclamide (*Glib*) (10 μM), a specific K_{ATP} channel inhibitor, further diminished the channel activity to the basal level. *B*, in the whole-cell recording, pinacidil-induced Kir6.2/SUR2B currents responded poorly to high concentrations of H_2O_2 (3 mM and 10 mM). *C*, in whole-cell configuration, the pinacidil-activated currents were potently inhibited by membrane-permeable 2-DTP (50 μM). *D*, in whole-cell configuration, membrane-impermeable DTNB (50 and 200 μM) had modest inhibitory effects on the Kir6.1/SUR2B channel activity. *E*, inside-out patch recording was obtained from an HEK cell expressing the Kir6.1/SUR2B channel with a holding potential of −60 mV. 2-DTP (3–30 μM) inhibited the pinacidil-induced Kir6.1/SUR2B channel progressively. *F*, increased doses of DTNB inhibited the Kir6.1/SUR2B channel in a similar manner. *G*, the effects of H_2O_2 (3 mM) on the Kir6.1/SUR2B and Kir6.2/SUR2B channels were compared. *H*, the dose-effect relationship of extracellular application of 2-DTP or DTNB with the activity of Kir6.1/SUR2B channel in the whole-cell configuration. *I*, the dose-effect relationship of 2-DTP or DTNB application with the activity of Kir6.1/SUR2B channel in inside-out patch configuration. ***, $p < 0.001$. *Error bars*, S.E.

0.05) (Fig. 2*A*). When both the N terminus and the core domain existed, the 112 had 2-DTP sensitivity (91.9 ± 8.0% inhibition; $n = 4$) as great as the 111 (Fig. 2*A*). This chimerical analysis thus suggests that both the N terminus and the core domain are crucial for the channel inhibition by 2-DTP.

Cys^{176} in the Kir6.1 Subunit—Systematic mutagenesis was carried out on all cysteine residues of the Kir6.1 (Fig. 3, *A* and *B*). All of the mutants exhibited functional channel activity when expressed with SUR2B in HEK cells. By 2-DTP screening, we found that one cysteine residue in the core domain (Cys^{176}) and another in the N terminus (Cys^{43}) were important, and mutations of these residues disrupted the channel sensitivity to 2-DTP (50 μM) in whole-cell recordings (Fig. 3, *B–D*). Mutation of any other cysteine residues did not result in a significant change in 2-DTP sensitivity using analysis of variance (Fig. 3*B*). Of these two cysteine residues, the Cys^{176} was more prominent in the oxidant-mediated channel inhibition because the Kir6.1-C176A/SUR2B channel lost most of its 2-DTP sensitivity (26.0 ± 6.5% inhibition, $p < 0.001$) (Fig. 3, *B* and *C*). Consistently, this mutant also lost its sensitivity to H_2O_2 (3.5 ± 4.7% inhibition; $p < 0.001$).

The Kir6.1-C176A mutant was further tested with GSSG, an *S*-glutathionylation inducer that modulates Kir6.1/SUR2B channel in inside-out patches (10, 30, 31). The WT Kir6.1/SUR2B channel was inhibited by GSSG drastically (84.3 ± 8.7% inhibition; $n = 5$) (Fig. 4*E*), whereas the Kir6.1-C176A/SUR2B channel was rather resistant to the GSSG treatments (17.8 ± 6.9% inhibition, $n = 4$, $p < 0.001$; Fig. 4, *A* and *E*). A treatment with 100 μM H_2O_2 in the presence of 100 μM GSH, another *S*-glutathionylation induction method (10), inhibited the Kir6.1-C176A mutant only marginally (14.7 ± 6.4% inhibition ($n = 4$); $p < 0.001$ compared with Kir6.1 WT) (Fig. 4, *B* and *F*) in inside-out patches. All of the results were consistent with the idea that Cys^{176} was a critical site for *S*-glutathionylation.

Cys^{43} and Cys^{120} in Oxidant Sensitivity—The Cys^{43} mutation (C43A) reduced the channel sensitivity to 50 μM 2-DTP (69.0 ± 3.8% inhibition; $n = 5$) (Fig. 3, *B* and *D*), although the effect was significantly smaller than that of Cys^{176} ($p < 0.001$). We further tested the effect of GSSG on the C43A mutation and found that the response of the Kir6.1-C43A mutant to GSSG was comparable with its response to 2-DTP, showing rather modest inhibition of the channel activity (60.9 ± 3.2% inhibition; $n = 4$) (Fig. 4, *C* and *E*). When the Kir6.1-C176A/C43A double mutation channel was tested, we found that the GSSG effect was completely eliminated (−3.9 ± 3.5% inhibition; $n = 4$) (Fig. 4, *D* and *E*).

In addition to Cys^{176} and Cys^{43}, Cys^{120} appeared to be important for the channel sensitivity to extracellular oxidants. The Kir6.1-C120S/SUR2B mutant channel lost substantial 2-DTP sensitivity (77.6 ± 5.1% inhibition; $n = 4$) (Fig. 3*E*), although

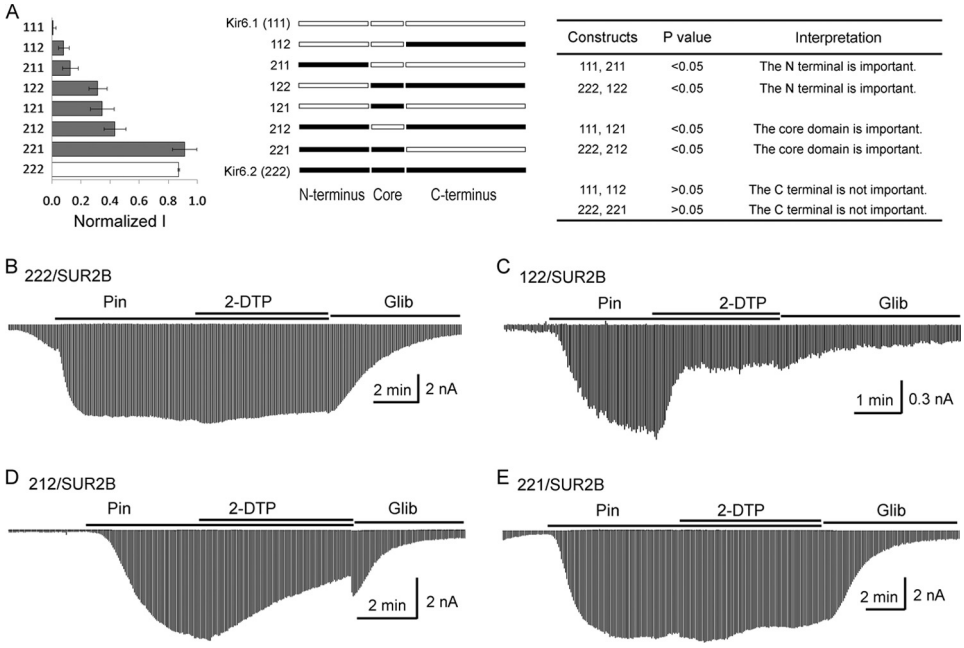

Constructs	P value	Interpretation
111, 211	<0.05	The N terminal is important.
222, 122	<0.05	The N terminal is important.
111, 121	<0.05	The core domain is important.
222, 212	<0.05	The core domain is important.
111, 112	>0.05	The C terminal is not important.
222, 221	>0.05	The C terminal is not important.

FIGURE 2. **The responses of chimerical channels to 2-DTP.** *A*, segments from Kir6.1 are shown in *white*, and segments from Kir6.2 are shown in *black*. The effect of 2-DTP (50 μM) on all of the chimerical channels is shown along with a *schematic diagram*. Compared with 111, both 211 and 121 showed decreased sensitivities to 2-DTP. Compared with 222, both 122 and 212 had stronger responses to 2-DTP treatments. Statistical analysis revealed that both the N terminus and the core domain were important for channel inhibition by 2-DTP. *B–E*, representative recordings demonstrated the responses of different constructs to treatment with 2-DTP. *Pin*, pinacidil; *Glib*, glibenclamide. *Error bars*, S.E.

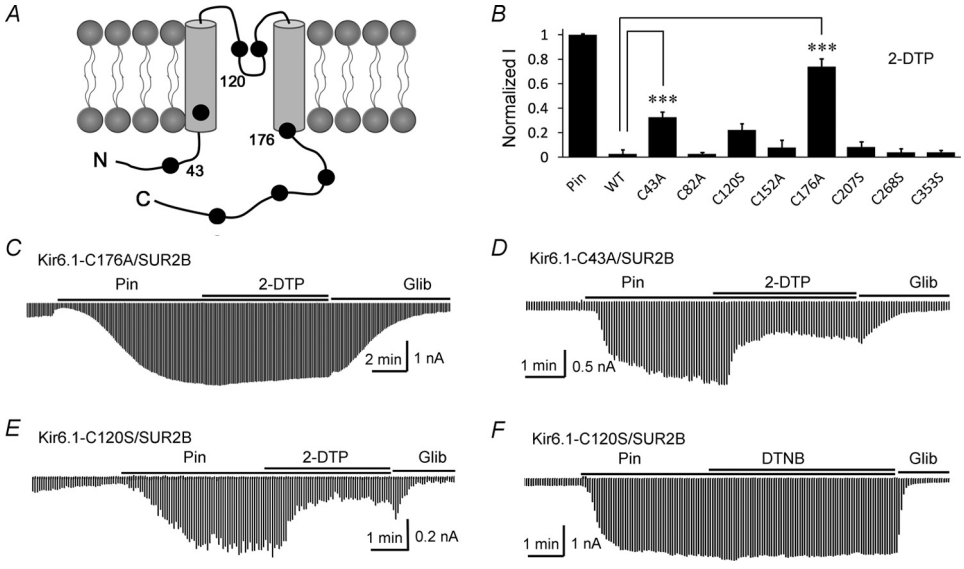

FIGURE 3. **Identification of the critical sites of cysteine modification.** *A*, *schematic diagram* of the approximate locations of the cysteine residues across the hKir6.1 subunit. *B*, summary of the effects of 2-DTP (50 μM) on the WT and mutant channels. Mutation of Cys^{43} and Cys^{176} showed impaired sensitivities to the 2-DTP (50 μM) treatment using analysis of variance. *C*, the Kir6.1-C176A/SUR2B mutant channel was activated by pinacidil (*Pin*). The current was resistant to the inhibitory effect of 2-DTP. Glibenclamide (*Glib*) still inhibited the channel activity. *D*, Kir6.1-C43A/SUR2B mutant channel showed impaired responses to 2-DTP-mediated channel inhibition. *E*, in another cell expressing the Kir6.1-C120S/SUR2B mutant channel, 2-DTP had a substantially inhibitory effect on the channel activity. *F*, Kir6.1-C120S/SUR2B currents were not sensitive to DTNB (200 μM), a membrane-impermeable PDS (***, $p < 0.001$). *Error bars*, S.E.

statistical significance was not found using analysis of variance. When the data were tested with Student's *t* test, however, its response to 2-DTP was significantly smaller than that of the Kir6.1/SUR2B WT channel ($p < 0.01$). Therefore, further studies were conducted on this site. In inside-out patches, the Kir6.1-Cys^{120} mutant did not show any reduction in its sensitivity to GSSG in comparison with Kir6.1/SUR2B WT channel (87.0 ± 5.8% inhibition ($n = 4$) *versus* 84.3 ± 8.7% inhibition ($n = 5$), respectively; $p > 0.05$) (Fig. 4*E*). When this mutant was examined in whole-cell recordings using membrane-impermeable DTNB (200 μM) applied extracellularly, the effect of DTNB was eliminated almost completely (2.7 ± 6.0% inhibition; $n = 6$) (Fig. 3*F*) in comparison with the Kir6.1/SUR2B WT channel (28.7 ± 5.2% inhibition by DTNB; $n = 5$) (Fig. 1*D*). These data thus suggest that Cys^{120} may serve for extracellular redox sensing but does not seem to be an *S*-glutathionylation site.

Biochemical Evidence for Cys^{176} Modification—Because Cys^{176} was the dominating residue mediating the *S*-glutathi-

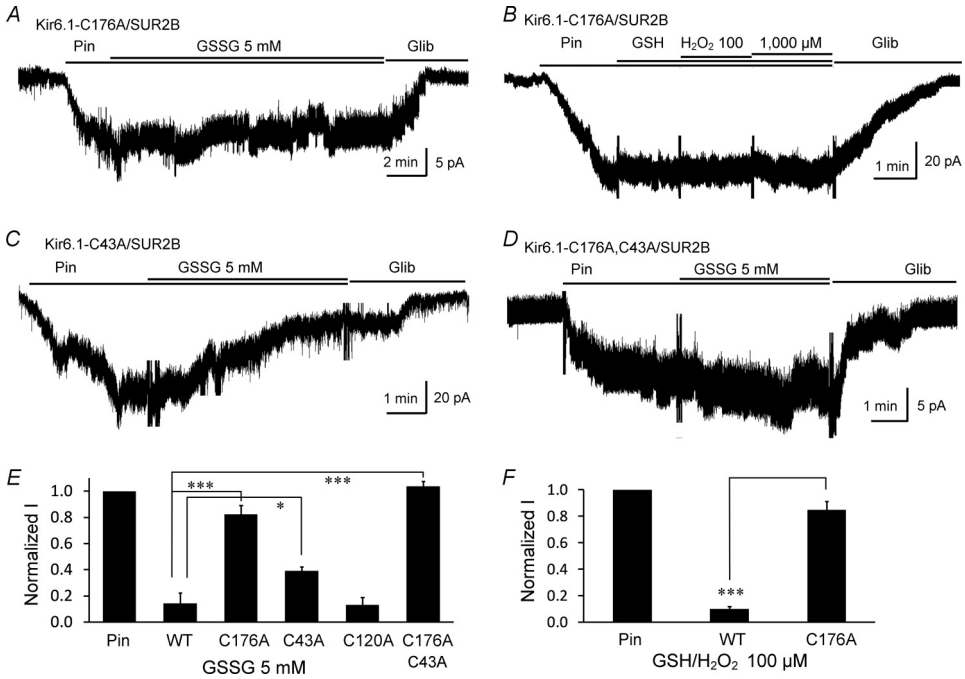

FIGURE 4. **The effect of *S*-glutathionylation on the WT and mutant channels.** *A*, in the Kir6.1-C176A/SUR2B mutant channel, 5 mM GSSG only had a slight inhibitory effect on the pinacidil-induced currents in giant inside-out patches. *B*, Kir6.1-C176A/SUR2B mutant channel was almost insensitive to the combined treatment of GSH and H_2O_2, another *S*-glutathionylation induction method. *C*, Kir6.1-C43A/SUR2B mutant channel was inhibited by GSSG (5 mM). *D*, Kir6.1-C43A/C176A/SUR2B channel was resistant to the inhibitory effect of GSSG. *E*, summary of the effects of GSSG on Cys^{176}, Cys^{43}, Cys^{120}, and Cys^{43}/Cys^{176} double mutants in giant inside-out patches ($n = 4–6$). *F*, summary of the effects of GSH/H_2O_2 on Kir6.1/SUR2B WT and Kir6.1-C176A/SUR2B mutant channels. *, $p < 0.05$; ***, $p < 0.001$. *Glib*, glibenclamide. *Pin*, pinacidil; *Error bars*, S.E.

onylation, we performed additional experiments to validate the essential role of Cys^{176} in *S*-glutathionylation biochemically. HEK cells transfected with WT channels or Kir6.1-C176A/SUR2B mutant were first tested for the expression of Kir6.1 protein. After cell lysis, anti-Kir6.1 antibodies detected strong Kir6.1-reactive bands in whole-cell extracts in both constructs. According to our previous study, a strong reactive band of ~32 kDa is Kir6.1-specific (10). The specificity of the antibodies is also confirmed by internal experiments performed by Sigma-Aldrich. With β-actin as loading control, we found that the density of the Kir6.1-C176A-reactive band was comparable with that of the Kir6.1 WT band (106 ± 8.5%; $n = 5$), indicating that the C176A mutation did not change the protein expression pattern of the Kir6.1 subunit (Fig. 5*A*). These constructs thus were subjected to a streptavidin pull-down assay. The HEK cells transfected with Kir6.1/SUR2B or Kir6.1-C176A/SUR2B were incubated with BioGEE (250 μM) for 1 h, followed by 15 min of H_2O_2 (750 μM) challenge as described previously (10, 32). If BioGEE was incorporated into the channel proteins, streptavidin-beads then should pull down the channel-BioGEE complex, which would be further detected by Kir6.1 antibodies in Western blot. On the other hand, if the mutation impaired the protein *S*-glutathionylation, then the mutation should decrease the binding of Kir6.1 protein to BioGEE, resulting in a weaker band or even no band in Western blot. Indeed, we observed different band densities between these two constructs. After streptavidin pull-down, the density of the Kir6.1-C176A-reactive band was much weaker (38.6 ± 3.8%; $n = 5$) (Fig. 5, *A* and *B*) compared with the band of the Kir6.1 WT channel after normalizing to protein inputs (Fig. 5, *A* and *B*). The data further

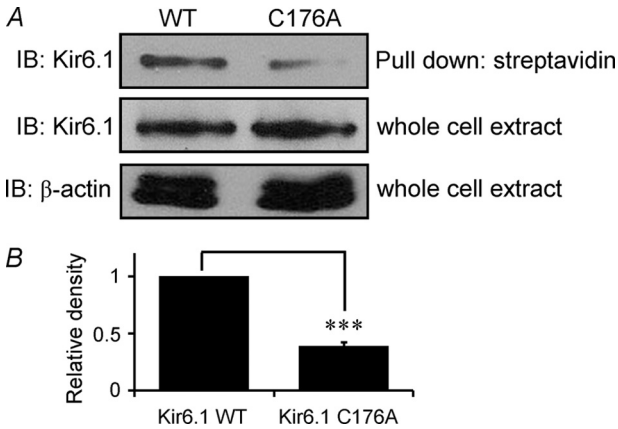

FIGURE 5. **Cys^{176} impaired the streptavidin pull-down.** *A*, whole-cell extracts were obtained from HEK cells expressing Kir6.1/SUR2B and Kir6.1-C176A/SUR2B channels using radioimmune precipitation assay buffer. The β-actin protein was detected using anti-β-actin antibodies as the loading control (*bottom*). The Kir6.1 proteins and Kir6.1-C176A mutant proteins were detected in the whole-cell extracts using anti-Kir6.1 antibodies. With the loading of the same amount of protein extracts, the anti-Kir6.1 antibodies detected bands of Kir6.1/SUR2B WT channel and Kir6.1-C176A/SUR2B mutant channel in a similar density (*middle*). The same amount of protein extracts (100 μg) from HEK293 cells expressing WT or mutant channels was subjected to the pull-down assay by the same amount of streptavidin beads (1 mg). Western blot using antibodies against Kir6.1 protein showed that the density of the Kir6.1-C176A-reactive band was much weaker compared with that of the Kir6.1 WT channel (*top*). *B*, the band densities of Kir6.1-C176A mutant channel after pull-down was normalized to that of Kir6.1 WT channel with the adjustment of inputs. Data were averaged from five individual repeats. ***, $p < 0.001$; *IB*, immunoblot; *error bars*, S.E.

demonstrate that the C176A mutation impaired the Kir6.1 protein *S*-glutathionylation.

As a control, the washout of the streptavidin bead-protein mixture was also used for Western blot. No clear bands were

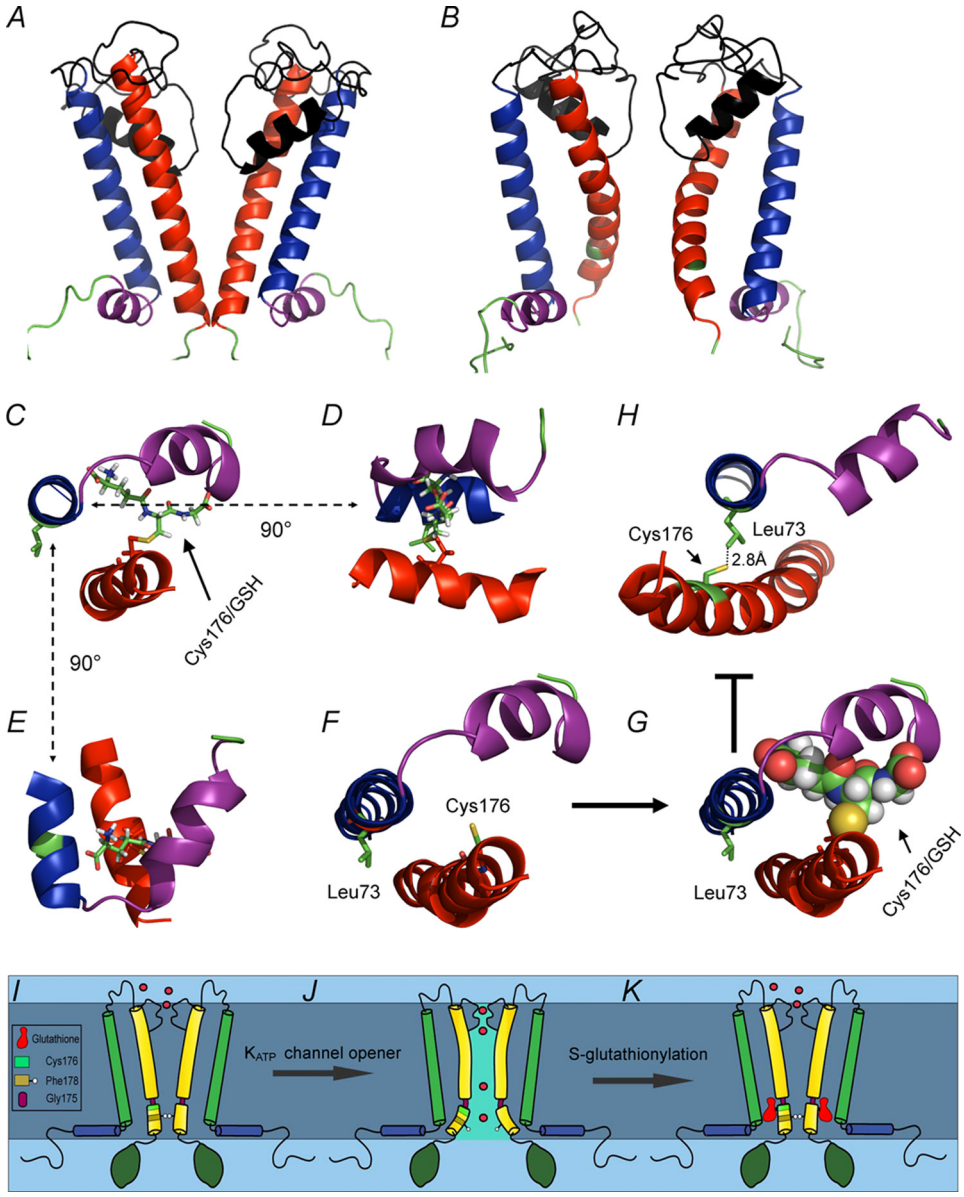

FIGURE 6. **Structural modeling of Kir6.1 *S*-glutathionylation at Cys^{176}.** *A*, structural modeling of the two opposing monomers of the Kir6.1 pore-forming domain in the closed state (the N and C termini are omitted for clarity; the whole structural model is shown in supplemental Fig. 1). *B*, structural model of the Kir6.1 pore-forming domain in its open state. *C–E*, *close-up views* of the GSH incorporated into Cys^{176} of the M2 inner helix. The location of GSH was determined by energy minimization. *D* and *E*, 90° turns of the view from *C*. *F* and *G*, intracellular view of the pore-lining helices of Kir6.1 (perpendicular to the axis of the M1 outer helix, *blue*) in the closed state model. Cys^{176} and Leu^{73} are shown in *sticks* (*G*, with a GSH moiety; *F*, without a GSH moiety). *H*, the same intracellular view of Kir6.1 in the open state model. Compared with *F*, the M2 inner helix (*red*) was bent leftward and twisted slightly, making Cys^{176} face directly toward the M1 outer helix (*blue*), where there was the residue Leu^{73}. The distance between the sulfur atom of Cys^{176} and the closest carbon atom of Leu^{73} was 2.8 Å in the open state compared with 9.2 Å in the closed state. Apparently, with the incorporation of a GSH moiety, this open conformation of the channel could not be achieved. Structural elements are *colored*: *blue*, M1 outer helix; *red*, M2 inner helix; *purple*, M0 slide helix; *black*, selectivity filter. GSH is shown in standard amino acid *colors*. The selectivity filter and connecting loops were removed in *C–H* for clarity. *I–K*, proposed models for *S*-glutathionylation-mediated channel gating. *I*, schematic view of K_{ATP} channel in its closed state. The "activation gate" Phe^{178} blocks the pore and prevents the ion from passing through. *J*, the administration of K_{ATP} channel opener causes a conformational change of K_{ATP} channel; the inner helix bends at Gly^{175} and moves the gate (Phe^{178}) away from the ion conduction pathway to facilitate the passage of potassium ions. *K*, *S*-glutathionylation at residue Cys^{176} results in the incorporation of GSH that occupies the space between the inner and outer helices. The addition of GSH prevents the channel from entering its open state.

detected in the washout from samples of either WT or mutant channels. This indicates that the Kir6.1 protein concentrations in the washout were below the threshold of detection by Western blot.

Simulation Modeling—Several Kir channel protein crystal structures, including the eukaryotic Kir2.2 channel structure, have been resolved recently. Although N and C termini show notable variation among different Kir channels, the core domains are rather conservative. To gain a structural insight into how the *S*-glutathionylation of Cys^{176} affects the channel activity, we modeled the Kir6.1 structure with a GSH moiety bound at residue 176 in its closed state (Fig. 6, *A* and *C–G*). Our model showed that after incorporation, the GSH moiety occupied the space between the M0, M1, and M2 helices (Fig. 6, *C–G*). The 360° view of the GSH-bound local structure is also presented (supplemental Fig. 1). Because the channel opening

requires a movement of the M2 inner helix (23, 25), the addition of GSH at residue Cys^{176} prevented the M2 inner helix from undergoing such a necessary movement for channel opening. To further validate this idea, we also modeled the Kir6.1 structure in its open state (Fig. 6, *B* and *H*) and compared it with the Kir6.1 model in its closed state. In the Kir6.1 open state model, the M2 inner helix was bent and twisted, making the Cys^{176} residue face the M1 outer helix directly (Fig. 6*H*). After energy minimization, the distance between Cys^{176} and the closest residue (Leu^{73}) on the M1 outer helix was 2.8 Å (Fig. 6*H*). When there was a GSH moiety on Cys^{176}, the channel open state with such a short distance between Cys^{176} and Leu^{73} could not be achieved. Consequently, the channel was retained in its closed state.

DISCUSSION

S-Glutathionylation is a post-translational modulation mechanism that is involved in a variety of physiological or pathophysiological events (33). We have recently shown that the VSM K_{ATP} channel, a vascular tone regulator, is modulated by *S*-glutathionylation. Our data in the present study reveal that the Kir6.1/SUR2B channel modulation by *S*-glutathionylation is likely to take place primarily at the Cys^{176} residue of the Kir6.1 subunit. Because of its critical location, the incorporation of the GSH moiety into Cys^{176} prevents the pore-forming inner helices from undergoing necessary conformational change for opening and retains the channel in its closed state.

Excessive reactive oxygen species produced during oxidative stress can result in structural modification of proteins affecting protein function (12). Although some studies have shown that the K_{ATP} channels are targeted by redox regulation, data are rather inconsistent regarding the effect of oxidants or thiol oxidation on K_{ATP} channels from different tissues. Reactive oxygen species lower the K_{ATP} channel activity in cerebral arterioles (34, 35) and coronary arteries (36) but facilitate its opening in cardiac myocytes (37) and pancreatic β-cells (38). Our results suggest that the differential responses of K_{ATP} channels to reactive oxygen species in these tissues are likely to be due to different isoforms of K_{ATP} channels expressed.

K_{ATP} channels consist of Kir6.1-containing channels and Kir6.2-containing channels. Although the Kir6.2 is the closest family member of Kir6.1, the intrinsic properties of these two groups of channels are quite different (39). For example, they have different biophysical properties and are modulated differently by PKA and PKC (40–42); the sensitivities of these channels to ATP and ADP are distinct (43); and without ATP, the Kir6.2 channel often opens automatically, whereas the Kir6.1 channel generally has low basal activity (16, 43, 44). Therefore, the studies of the Kir6.2 channel often take the advantage of its automatic opening, whereas the studies of the Kir6.1 channel require the K_{ATP} channel openers to activate the channel. In this current study, we found another major difference between these channels. The Kir6.1/SUR2B channel is inhibited by oxidants and reactive disulfides strongly, whereas the Kir6.2/SUR2B channel is barely inhibited by these reagents. These different responses may be attributable to the difference between Kir6.1 and Kir6.2 subunits. However, we cannot rule out the possibility of the involvement of the SUR subunit. The close coupling between Kir6.x and SURx is well recognized. The SUR is known to interact with the N terminus but not the C terminus of Kir6.x to affect channel gating (45, 46). Such an interaction may rely on certain N-terminal residues and produce different conformational supports for distinct Kir6.x subunits. However, our data do suggest that the cysteine residues in the SUR2B subunit are not functionally *S*-glutathionylated, which is supported by our systematic mutagenesis for all the intracellular cysteine residues in the SUR2B subunit (supplemental Fig. 2).

Previous studies of the oxidant sensitivity of K_{ATP} channels were mainly focused on Kir6.2-containing channels (2). Studies of Kir6.2-containing channels in native tissues suggest that the application of H_2O_2 facilitates the opening of these channels, preferentially through changing the ATP/ADP sensitivity of the Kir6.2-containing channels (38, 47). On the other hand, Kir6.2ΔC26 (truncated Kir6.2 that can express by itself) or Kir6.2 with SUR1 is inhibited by *p*-chloromercuriphenylsulfonate, a sulfhydryl-modifying reagent. Further investigations have shown that Cys^{42} (the corresponding site of Cys^{43} in Kir6.1) is the major site involved in the channel inhibition (44). Consistently, we have also found Cys^{43} in Kir6.1, the counterpart of Cys^{42} in Kir6.2, to be modulated by exogenous thiol oxidants. More importantly, this residue in Kir6.1 appears to be a *S*-glutathionylation site, although it does not seem to play a leading role compared with Cys^{176}.

Biochemical experiments, including Western blot and pull-down assays, require the use of Kir6.1 antibodies. Kir6.1 antibodies have been generated from different laboratories and are also commercially available. Interestingly, although specific, antibodies from different sources detect bands of distinct sizes in different tissue samples. For example, a single band of 35, 44, or 49 kDa has been detected in rat heart tissue from three independent studies (48–50), respectively. In rat brain samples, a single band of 51 kDa has been detected (48), whereas another study has detected the Kir6.1 band between 37 and 50 kDa in adult mouse hippocampus (51). In the present study, we used the Kir6.1 antibodies purchased from Sigma-Aldrich. The size of the Kir6.1-reactive band detected in our study is close to the band detected from heart tissue by Sun *et al.* (48). It is suggested that the post-translational modification, the natural truncation of Kir6.1 protein during the preparation, and the methods of sample treatment (*e.g.* lysis reagents, reducing or non-reducing preparation, etc.) may affect the size of Kir6.1 protein from different tissues.

K_{ATP} channels have been modeled previously using crystallized bacterial channels as templates (52–55). In this study, the closed state of the Kir6.1 is modeled using the most recently crystallized eukaryotic Kir2.2 together with bacterial Kir channels as templates (see supplemental Fig. 3 for sequence alignments). The open state model is generated based on the open state KirBac1.1 structural model provided by Dr. Venien-Bryan (25, 26). With the information from these structures, a model of the *S*-glutathionylation-mediated Kir6.1/SUR2B channel gating is proposed (Fig. 6, *I–K*, and supplemental Movie 1). A conservative phenylalanine residue (Phe^{146} of KirBac1.1; Phe^{178} of Kir6.1) located in the narrowest region of the ion conduction pathway is likely to serve as "blocking residue/activation gate" that prevents K^+

from passing through when the channel is closed (23, 56). When the channel is open, the slide helix moves laterally and exerts strain on the bottom of the inner helix, resulting in the bending of the inner helix at a weak point (*e.g.* a glycine residue (Gly^{175} of Kir6.1)). This bending moves the side chain of the blocking residue (Phe^{178} of Kir6.1) away from the center of the ion conduction pathway and allows K^+ to pass through (25). In the channel open state, Cys^{176} of the M2 helix makes a close contact with the M1 helix. The closest distance between Cys^{176} and Leu^{73} in the M1 helix is measured to be 2.8 Å. Such a short distance/small space cannot accommodate a GSH moiety (or even a smaller thiol modulation regent, 2-DTP). Therefore, when the channel is *S*-glutathionylated, the open conformation of the channel cannot be achieved.

In the Kir6.2 channel, Cys^{166} (corresponding to Cys^{176} in Kir6.1) is suggested to be involved in the intrinsic channel gating (57). The channel with the C166S mutation lost most of its sensitivity to both K_{ATP} channel opener and inhibitor with a drastic augmentation of the channel open probability (57). However, Cys^{176} in the Kir6.1/SUR2B channel does not seem to be a general gating site. We have found that Kir6.1/SUR2B channels with the C176A mutation are still sensitive to both K_{ATP} channel opener and inhibitor, indicating that the general channel gating machinery of Kir6.1/SUR2B channel is still intact with the Cys^{176} mutation.

In contrast to the conserved core domain, the N terminus of the Kir channel shows considerable variations (supplemental Fig. 3). The crystal structure of the N terminus of Kir channels cannot be modeled with a decent resolution. Therefore, we did not attempt to study how the *S*-glutathionylation of Cys^{43} affects the protein conformation.

Unlike Cys^{176} and Cys^{43}, Cys^{120} does not seem to be involved in *S*-glutathionylation. In the Kir2.1 channel, the mutation of Cys^{122}, the counterpart of Cys^{120} in Kir6.1, results in an absence of ionic currents although the channels are still expressed (58, 59). In our studies, we were able to record the currents from the C120S mutant, although the currents were rather small compared with most of the other mutants. Based on the Kir protein structure, Cys^{120} is located on the extracellular interface of the cellular membranes, accessible to extracellular environments. The accessibility of this residue to extracellular oxidants as well as membrane-impermeable PDS, but not intracellular GSSG, suggests that Cys^{120} could be a site for extracellular redox modulation rather than intracellular *S*-glutathionylation.

In conclusion, our studies indicate that *S*-glutathionylation inhibits the Kir6.1/SUR2B channel by targeting mainly Cys^{176} of the Kir6.1 subunit. *S*-Glutathionylation at Cys^{176} is likely to structurally prevent the pore-forming inner helix from undergoing necessary conformational change for channel gating, thus retaining the channel in its closed state. The demonstration of the molecular mechanism underlying *S*-glutathionylation of the vascular K_{ATP} channel with structural insight into the channel gating should have a profound impact on the understanding of the post-translational modifications of ion channels.

Acknowledgments—We are grateful to Dr. Yang Zhang and Ambrish Roy at the University of Michigan for help and comments on the Kir6.1 structural models. We acknowledge Dr. Susumu Seino at Kobe University for the gift of Kir6.1 and Kir6.2 cDNA as well as Dr. Yoshihisa Kurachi at Osaka University for the SUR2B cDNA.

REFERENCES

1. Nichols, C. G. (2006) *Nature* **440,** 470–476
2. Yokoshiki, H., Sunagawa, M., Seki, T., and Sperelakis, N. (1998) *Am. J. Physiol.* **274,** C25–C37
3. Miki, T., and Seino, S. (2005) *J. Mol. Cell Cardiol.* **38,** 917–925
4. Seino, S. (1999) *Annu. Rev. Physiol.* **61,** 337–362
5. Teramoto, N. (2006) *J. Physiol.* **572,** 617–624
6. Miki, T., Suzuki, M., Shibasaki, T., Uemura, H., Sato, T., Yamaguchi, K., Koseki, H., Iwanaga, T., Nakaya, H., and Seino, S. (2002) *Nat. Med.* **8,** 466–472
7. Chutkow, W. A., Pu, J., Wheeler, M. T., Wada, T., Makielski, J. C., Burant, C. F., and McNally, E. M. (2002) *J. Clin. Invest.* **110,** 203–208
8. Croker, B., Crozat, K., Berger, M., Xia, Y., Sovath, S., Schaffer, L., Eleftherianos, I., Imler, J. L., and Beutler, B. (2007) *Nat. Genet.* **39,** 1453–1460
9. Kane, G. C., Lam, C. F., O'Cochlain, F., Hodgson, D. M., Reyes, S., Liu, X. K., Miki, T., Seino, S., Katusic, Z. S., and Terzic, A. (2006) *FASEB J.* **20,** 2271–2280
10. Yang, Y., Shi, W., Cui, N., Wu, Z., and Jiang, C. (2010) *J. Biol. Chem.* **285,** 38641–38648
11. Dalle-Donne, I., Rossi, R., Colombo, G., Giustarini, D., and Milzani, A. (2009) *Trends Biochem. Sci.* **34,** 85–96
12. Dalle-Donne, I., Rossi, R., Giustarini, D., Colombo, R., and Milzani, A. (2007) *Free Radic. Biol. Med.* **43,** 883–898
13. Shi, W., Cui, N., Shi, Y., Zhang, X., Yang, Y., and Jiang, C. (2007) *Am. J. Physiol. Regul. Integr. Comp. Physiol.* **293,** R191–R199
14. Shi, W., Cui, N., Wu, Z., Yang, Y., Zhang, S., Gai, H., Zhu, D., and Jiang, C. (2010) *J. Biol. Chem.* **285,** 3021–3029
15. Shi, Y., Chen, X., Wu, Z., Shi, W., Yang, Y., Cui, N., Jiang, C., and Harrison, R. W. (2008) *J. Biol. Chem.* **283,** 7523–7530
16. Shi, Y., Cui, N., Shi, W., and Jiang, C. (2008) *J. Biol. Chem.* **283,** 2488–2494
17. Shi, Y., Wu, Z., Cui, N., Shi, W., Yang, Y., Zhang, X., Rojas, A., Ha, B. T., and Jiang, C. (2007) *Am. J. Physiol. Regul. Integr. Comp. Physiol.* **293,** R1205–R1214
18. Yang, Y., Shi, Y., Guo, S., Zhang, S., Cui, N., Shi, W., Zhu, D., and Jiang, C. (2008) *Biochim. Biophys. Acta* **1778,** 88–96
19. Zhang, Y. (2008) *BMC Bioinformatics* **9,** 40
20. Roy, A., Kucukural, A., and Zhang, Y. (2010) *Nat. Protoc.* **5,** 725–738
21. Zhang, Y. (2009) *Proteins* **77,** Suppl. 9, 100–113
22. Nishida, M., Cadene, M., Chait, B. T., and MacKinnon, R. (2007) *EMBO J.* **26,** 4005–4015
23. Kuo, A., Gulbis, J. M., Antcliff, J. F., Rahman, T., Lowe, E. D., Zimmer, J., Cuthbertson, J., Ashcroft, F. M., Ezaki, T., and Doyle, D. A. (2003) *Science* **300,** 1922–1926
24. Tao, X., Avalos, J. L., Chen, J., and MacKinnon, R. (2009) *Science* **326,** 1668–1674
25. Kuo, A., Domene, C., Johnson, L. N., Doyle, D. A., and Vénien-Bryan, C. (2005) *Structure* **13,** 1463–1472
26. Domene, C., Doyle, D. A., and Vénien-Bryan, C. (2005) *Biophys. J.* **89,** L01–L03
27. Harrison, R. W., and Weber, I. T. (1994) *Protein Eng.* **7,** 1353–1363
28. Cao, K., Tang, G., Hu, D., and Wang, R. (2002) *Biochem. Biophys. Res. Commun.* **296,** 463–469
29. Tricarico, D., Mele, A., Lundquist, A. L., Desai, R. R., George, A. L., Jr., and Conte Camerino, D. (2006) *Proc. Natl. Acad. Sci. U.S.A.* **103,** 1118–1123
30. Kil, I. S., Kim, S. Y., and Park, J. W. (2008) *Biochem. Biophys. Res. Commun.* **373,** 169–173
31. Wang, W., Oliva, C., Li, G., Holmgren, A., Lillig, C. H., and Kirk, K. L. (2005) *J. Gen. Physiol.* **125,** 127–141
32. Zmijewski, J. W., Banerjee, S., and Abraham, E. (2009) *J. Biol. Chem.* **284,** 22213–22221

33. Mieyal, J. J., Gallogly, M. M., Qanungo, S., Sabens, E. A., and Shelton, M. D. (2008) *Antioxid. Redox Signal.* **10,** 1941–1988
34. Erdös, B., Simandle, S. A., Snipes, J. A., Miller, A. W., and Busija, D. W. (2004) *Stroke* **35,** 964–969
35. Ross, J., and Armstead, W. M. (2003) *Am. J. Physiol. Regul. Integr. Comp. Physiol.* **285,** R149–R154
36. Miura, H., Wachtel, R. E., Loberiza, F. R., Jr., Saito, T., Miura, M., Nicolosi, A. C., and Gutterman, D. D. (2003) *Circ. Res.* **92,** 151–158
37. Tokube, K., Kiyosue, T., and Arita, M. (1998) *Pflugers Arch.* **437,** 155–157
38. Krippeit-Drews, P., Kramer, C., Welker, S., Lang, F., Ammon, H. P., and Drews, G. (1999) *J. Physiol.* **514,** 471–481
39. Hibino, H., Inanobe, A., Furutani, K., Murakami, S., Findlay, I., and Kurachi, Y. (2010) *Physiol. Rev.* **90,** 291–366
40. Thorneloe, K. S., Maruyama, Y., Malcolm, A. T., Light, P. E., Walsh, M. P., and Cole, W. C. (2002) *J. Physiol.* **541,** 65–80
41. Light, P. E., Bladen, C., Winkfein, R. J., Walsh, M. P., and French, R. J. (2000) *Proc. Natl. Acad. Sci. U.S.A.* **97,** 9058–9063
42. Lin, Y. F., Jan, Y. N., and Jan, L. Y. (2000) *EMBO J.* **19,** 942–955
43. Farzaneh, T., and Tinker, A. (2008) *Cardiovasc. Res.* **79,** 621–631
44. Trapp, S., Tucker, S. J., and Ashcroft, F. M. (1998) *J. Gen. Physiol.* **112,** 325–332
45. Babenko, A. P., and Bryan, J. (2003) *J. Biol. Chem.* **278,** 41577–41580
46. Babenko, A. P., and Bryan, J. (2002) *J. Biol. Chem.* **277,** 43997–44004
47. Ichinari, K., Kakei, M., Matsuoka, T., Nakashima, H., and Tanaka, H. (1996) *J. Mol. Cell Cardiol.* **28,** 1867–1877
48. Sun, X., Cao, K., Yang, G., Huang, Y., Hanna, S. T., and Wang, R. (2004) *Biochem. Pharmacol.* **67,** 147–156
49. Akao, M., Otani, H., Horie, M., Takano, M., Kuniyasu, A., Nakayama, H., Kouchi, I., Murakami, T., and Sasayama, S. (1997) *J. Clin. Invest.* **100,** 3053–3059
50. Morrissey, A., Rosner, E., Lanning, J., Parachuru, L., Dhar Chowdhury, P., Han, S., Lopez, G., Tong, X., Yoshida, H., Nakamura, T. Y., Artman, M., Giblin, J. P., Tinker, A., and Coetzee, W. A. (2005) *BMC Physiol.* **5,** 1
51. Soundarapandian, M. M., Wu, D., Zhong, X., Petralia, R. S., Peng, L., Tu, W., and Lu, Y. (2007) *J. Neurochem.* **103,** 1982–1988
52. Proks, P., and Ashcroft, F. M. (2009) *Prog. Biophys. Mol. Biol.* **99,** 7–19
53. Bichet, D., Haass, F. A., and Jan, L. Y. (2003) *Nat. Rev. Neurosci.* **4,** 957–967
54. Bryan, J., Vila-Carriles, W. H., Zhao, G., Babenko, A. P., and Aguilar-Bryan, L. (2004) *Diabetes* **53,** Suppl. 3, S104–S112
55. Antcliff, J. F., Haider, S., Proks, P., Sansom, M. S., and Ashcroft, F. M. (2005) *EMBO J.* **24,** 229–239
56. Rojas, A., Wu, J., Wang, R., and Jiang, C. (2007) *Biochim. Biophys. Acta* **1768,** 39–51
57. Trapp, S., Proks, P., Tucker, S. J., and Ashcroft, F. M. (1998) *J. Gen. Physiol.* **112,** 333–349
58. Cho, H. C., Tsushima, R. G., Nguyen, T. T., Guy, H. R., and Backx, P. H. (2000) *Biochemistry* **39,** 4649–4657
59. Leyland, M. L., Dart, C., Spencer, P. J., Sutcliffe, M. J., and Stanfield, P. R. (1999) *Pflugers Arch.* **438,** 778–781